



# The influence of the structural distribution and hardness of mineral phases on the size and shape of rock drilling particles

Xiaofeng Yang<sup>a</sup>, Aiguo Nie<sup>a</sup>, Derek Elsworth<sup>b</sup> and Jiaheng Zhou<sup>a</sup>

<sup>a</sup>School of Mechanics and Civil Engineering, China University of Mining and Technology, Beijing, China; <sup>b</sup>Department of Energy and Mineral Engineering, EMS Energy Institute and G3 Center, Pennsylvania State University, University Park, PA, USA

## ABSTRACT

Rock drilling is a significant activity widely used in the exploration of marine mineral resources and offshore civil engineering such as marine mining, petroleum and deep-water drilling. The characteristics of size and shape of particles produced during rock drilling influence drilling efficiency and energy consumption. We report a series of drilling experiments on sandstone, limestone and shale to systematically examine particle size distribution and shape and correlate these with original rock structure and composition. Correlations are established via metrics of particle size distribution, average circularity and specific surface area. Impact breakage and contact abrasion of individual particles during rock drilling are the main mechanisms controlling particle size and shape. Impact breakage is controlled by the structural distribution of mineral phases, while contact abrasion is principally related to the hardness of mineral phases. The particle size distribution is affected by the structural distribution of mineral phases. The average circularity of the drilling particles is mainly controlled by the hardness of mineral phases. The specific surface area of rock drilling particles is determined by both structural distribution and hardness of mineral phases – with homogeneous structure and low average hardness of the phases reducing the resulting specific surface area of the drilling products.

## ARTICLE HISTORY

Received 2 February 2020  
Accepted 12 March 2020

## KEYWORDS

Rock drilling particles; characteristics of mineral phases; particle size distribution; circularity; specific surface area

## 1. Introduction

Rock drilling is an engineering activity widely used in the exploration and development of marine mineral resources and offshore civil engineering such as marine mining, petroleum, deep-water drilling and foundation. (Liu et al. 2016; Zhou et al. 2017; Harper and Chambers 2004). There are limits to improving drilling efficiency from the perspective of tool materials, structure and design (Miyazaki et al. 2016; Ren, Miao, and Peng 2013; Flegner et al. 2016; Spagnoli, Bosco, and Oreste 2016) and in optimizing operational parameters (Ersoy and Waller 1997). Rock drilling is an intrinsically complex process involving dynamics, rock mechanics, material tribology and fluid mechanics. Thus, it is necessary to take advantage of further perspectives to study the underlying mechanisms in the drilling process (Che, Zhu, and Ehmann 2016; Wu and Han 2009; Bondarenko et al. 2013; Xu et al. 2018).

The creation of comminuted particles plays a significant role in the drilling process via rock crushing and fracture (Akhshik, Behzad, and Rajabi 2016; Nascimento et al. 2019; You et al. 2018; Tavares 2004). Furthermore, the specific surface area of milled limestone particles typically increases with an increase in revolution speed for a prescribed grinding duration (Guzzo, Tino, and Santos 2015). An increase in

the size of the drilling particles intensifies wear of the drill bit (Weichert 1991), with the angularity and concavity of particles strongly correlated with the wear rate (Pellegrin et al. 2009). The experiments on the effect of particle shape on heat transfer of sand demonstrates that particle with a higher average value of sphericity and roundness show a tendency to boost higher thermal conductivity. (Fei, Narsilio, and Disfani 2019). Simulation results indicate that the higher the sphericity of rock breaking particles, the lower the consumption of surface energy and specific energy (Dunatunga and Kamrin 2017). The required input energy increases exponentially for an increase in total surface area of the comminuted coal particles, and the specific surface energy is not constant but related to the physical properties of coal (Luo et al. 2018). Numerical simulations of impact-loaded concrete and coal demonstrate that mean particle size is non-linearly negatively correlated with the impact energy (Tavares 1999; Whittles et al. 2006; Reddish et al. 2005; Krauthammer et al. 2003).

The form and distribution of rock drilling particles produced during drilling provide important insights into breakage mechanisms and the influence of rock type and structure on drilling efficiency. These impacts are poorly constrained, with the following systematically exploring such

**Table 1.** Mechanical and physical properties of the rock material.

	Compressive strength (MPa)	Shear strength (MPa)	Friction angle (°)	Density (g/cm <sup>3</sup> )
Sandstone	60.73	18.9	55	2.47
Limestone	145.40	14.7	67	2.50
Shale	192.91	57.8	65	2.55

controls on the rock drilling process. Towards this goal, laboratory drilling experiments are completed at variable rotation and penetration rates on sandstone, limestone and shale and the full particle size distribution (PSD), morphology and compositions of the drilling particles are measured. These observations are used to define the main factors controlling the morphology of the comminution products and to probe key mechanisms of breakage.

## 2. Materials and experimental methods

A series of rock drilling experiments are conducted using limestone, sandstone and shale specimens collected from the Mentougou Mine, west of Beijing, for which material parameters were measured by the uniaxial compression test, shear test and rock densitometer, as shown in Table 1.

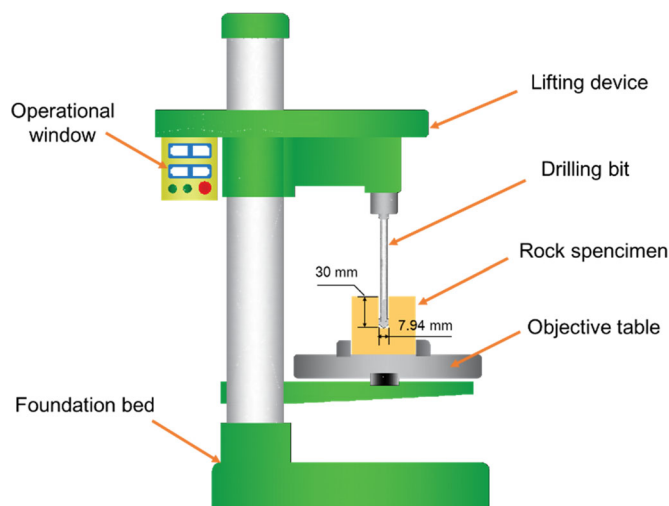
The drilling experiments were conducted in a bench drilling system (1kW, Z3040, made by Zhongjie Drilling Machine Factory), as shown in Figure 1. The blade of the auger bit was carbide YG8, with a diameter of 7.94 mm. The two experimental variables were the rotation rate and the penetration rate with each parameter specified at 5 levels (Table 2). A full suite of drilling experiments was completed under each rotation and penetration rate, with each rotation rate matched to 5 penetration rates – resulting in a total of 25 drilling tests, each 30 mm in depth.

The Particle size distributions and average specific surface area of the resulting particles were measured in a Malvern Mastersizer 3000 with the morphology and circularity of particles obtained from a Malvern Morphologi. Compositions of the particles were defined by X-ray powder diffraction (Cu-target, Rigaku TTRIII), with the micro-structure of the three rock specimens observed on thin sections by polarizing microscope. Mineral compositions were provided by Electron Probe Micro Analysis (GENESIS XM, EDAX).

## 3. Results and discussion

### 3.1. The influence of the structural distribution and hardness of mineral phases on the particle size distribution in rock drilling

The PSD curves of the drilling particles recovered from all experiments on the three types of rocks is comparatively analyzed. For all three rock types, the particle sizes are principally distributed in the range 1–1000  $\mu\text{m}$  – identified as medium (1–75  $\mu\text{m}$ ) to coarse (>75  $\mu\text{m}$ ). The PSDs of all three rock types are broadly similar but exhibit specific distinctive features for each rock type. Figure 2 shows two peaks (Peak I of the fine fraction and

**Figure 1.** Rock drilling system.**Table 2.** Operational parameters for the drilling experiments.

Penetration rate (mm/s)	0.75	0.85	1.00	1.20	1.50
Rotation rate (rpm)	600	900	1250	1750	2600

Peak II of the coarse fraction) in the PSD curves for limestone and sandstone, however, there is only a single peak for the PSD of shale.

In the drilling process, interaction between the particles reshapes them. The particle size and shape are mainly influenced by the effects of both impact breakage and contact abrasion between the rock particles (Figure 3). The effect of impact breakage causes larger particles to break up into several smaller ones – resulting in a decrease in particle size and circularity (Figure 3a). While the effect of contact abrasion causes the polishing of particles and the removal of edges and vertices, resulting in an increase in circularity (Figure 3b) and a concomitant decrease in surface area.

Drilling operational parameters affect the severity of both impact breakage and contact abrasion – higher rotation rates could contribute to increased impact breakage and larger penetration rates to increased contact abrasion. However, the compositional characteristics of rock also influence these mechanisms of comminution.

Table 3 shows the distinctions in minerals contents between the sandstone, limestone and shale particles. The results of EPMA analysis indicate that the sandstone and limestone comprise individual grains (I in Figure 4a, b) separated by infilling cements (II in Figure 4a, b). The majority volume is of individual grains, comprising mono-mineralic quartz and calcite with infilling cements comprising clay minerals such as kaolinite and illite. This structural distribution can be referred to as a two-phase structure. By contrast, the composition of the shale is of uniformly and closely packed small grains absent infilling cements (Figure 4c). This structural distribution may be referred to as a single-phase or homogeneous structure.

The shale has a homogeneous structure with a uniform array of dense components. This induces initial breakage of

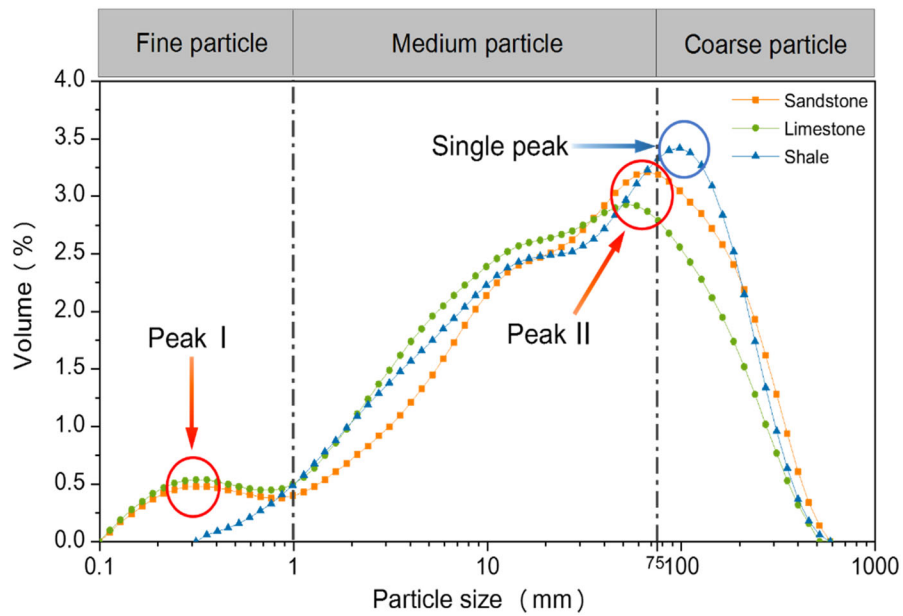


Figure 2. Typical PSD curves for drilling products from sandstone, limestone and shale penetrated at 1.50 mm/s for a rotation rate of 1750 rpm.

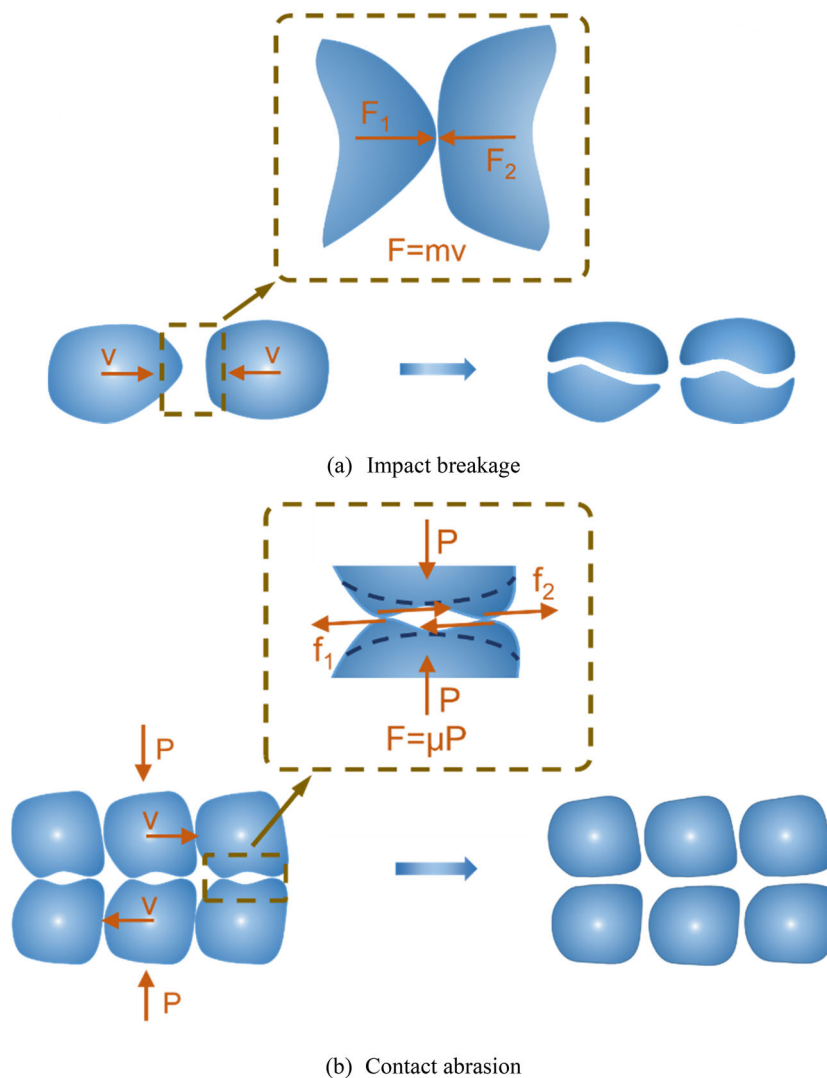


Figure 3. Interaction modes between particles. (a) Impact breakage: Initially non-contacting particles with high momentum approach each other, where  $v$  is the velocity of the particle,  $F$  is the impact force,  $m$  is the particle mass; (b) Contact abrasion: Contacting particles move in shear relative to each other, where  $P$  is the contact force caused by particles above and below,  $f$  is the surface friction, and  $\mu$  is the friction coefficient.

**Table 3.** XRD analysis for particles derived from the three rock types.

Mineral	Mohs hardness	Contents (%)		
		Sandstone	Limestone	Shale
Quartz	7	93.0	52.0	26.9
Plagioclase	6.5	—	8.2	0.6
Calcite	3	—	23.7	23.7
Dolomite	3.5	—	—	39.4
Pyrite	6	—	—	1.6
Clay minerals	2.5	7.0	16.1	7.8

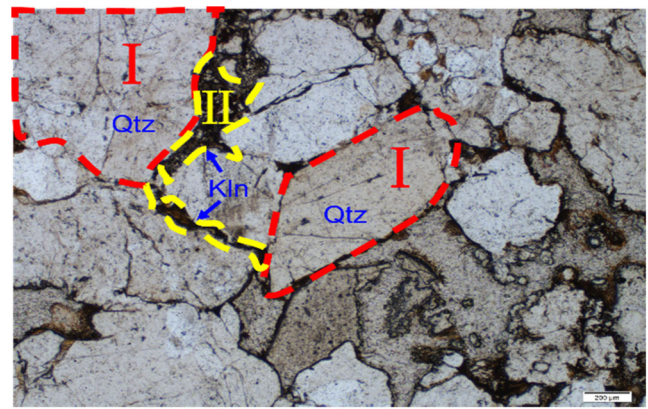
particles with similar hardness on internal cleavage surfaces avoiding impact breakage. Thus, a single peak (in the coarse particle fraction) results in the PSD curve for shale. However, both limestone and sandstone have a two-phase structure – the interfaces separating the phases are fragile and readily break into the two component phases with different hardnesses, as a result of impact breakage. Subsequently, the low-hardness phases are readily broken into smaller particles, and concentrate as a prominent fine peak (Peak I – fine particle fraction), while the high-hardness particles resist breakage and are manifest as Peak II (coarse particle fraction) as shown in Figure 2.

### 3.2. The influence of the structural distribution and hardness of mineral phases on the average circularity of the rock drilling particle

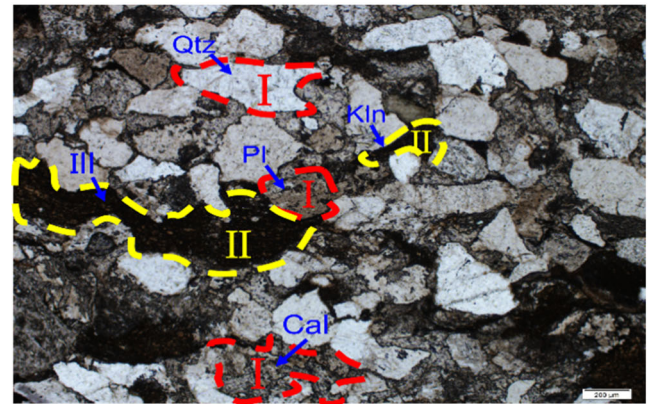
The 2D projections of the particles which reflect shape and circularity are obtained by the Malvern Morphologi (Figure 5) classifier. The distribution of average circularity and the quartz content of particles from the three rock types over all drilling experiments are statistically shown as boxplots in Figure 6.

The range of average circularity of the shale is the largest, that of sandstone is smallest, with limestone intermediate between these. Meanwhile, Figure 6 also shows quartz contents, with shale the smallest, sandstone the largest, with limestone intermediate. So the particle circularity is obviously inverse to quartz content. Thus, quartz content significantly affects the range of average circularity of the rock drilling particles with quartz grains less affected by the effects of impact breakage and contact abrasion induced due to its high hardness. Therefore, high quartz content could contribute to reducing the range in magnitudes of average circularity.

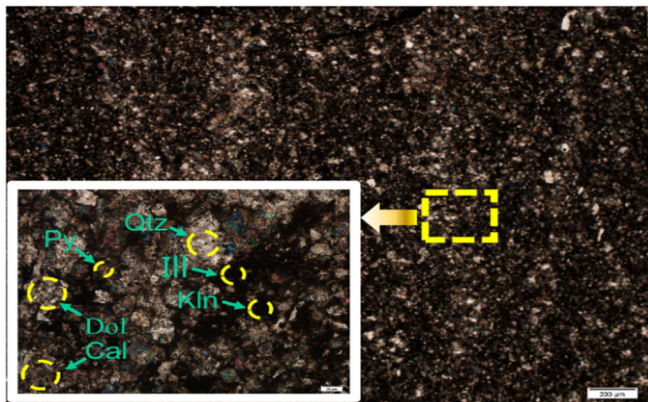
The median value of the average circularity in the shale is much larger than that of limestone and sandstone (Figure 6). Pyrite in shale may decompose into iron and sulfur as a result of the high drilling temperature. The oxidized iron and sulfur attached to the particle surface will reduce the surface hardness and intensify contact abrasion prompting an increase in particle circularity. In addition, the hardness of the mineral phases affects contact abrasion. The volume-averaged hardness of the phases may be used as an index for the rocks. According to Table 3, the average Mohs hardness of the phase of sand is 6.65, that of limestone is 5.17 and shale is 4.26. The average hardness of the phases for



(a) Sandstone



(b) Limestone



(c) Shale

**Figure 4.** Polarizing microscope images and EPMA for the three rock types. (a) Sandstone; (b) limestone; (c) shale (Qtz-quartz, Py-pyrite, Pl-plagioclase, Ill-illite, Kln-kaolinite, Dol-dolomite, Cal-calcite).

shale is the lowest, resulting in the highest level of contact abrasion to contribute to an increase in its particle circularity.

### 3.3. The influence of the structural distribution and hardness of mineral phases on specific surface area of the rock drilling particle

The average specific surface area of particles derived from the three rock types are similarly high for sandstone and

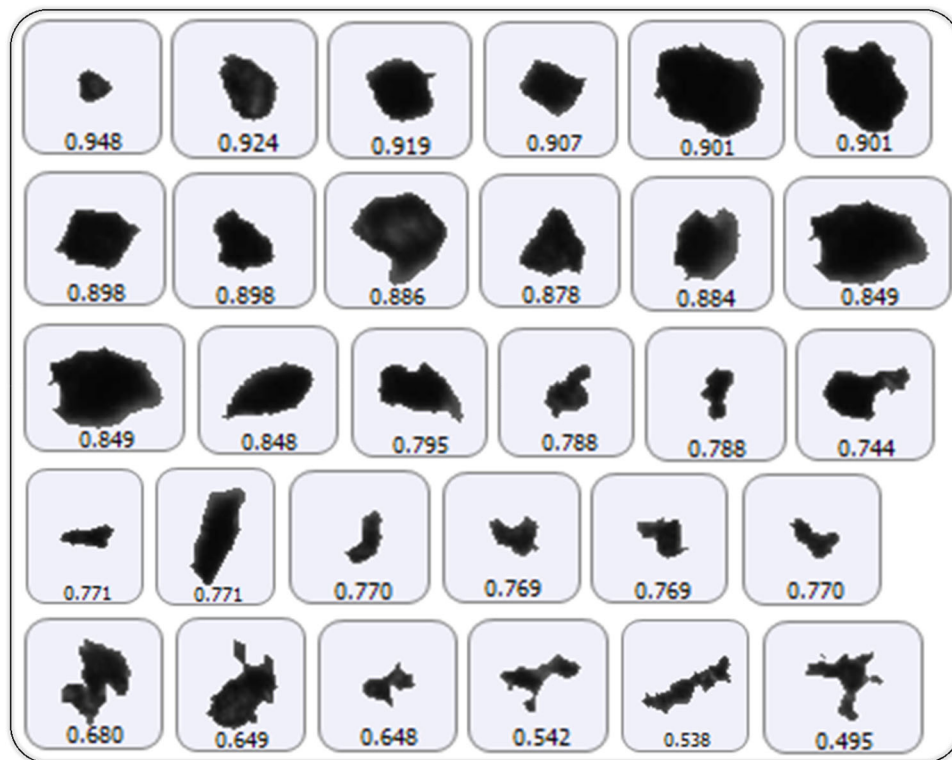


Figure 5. Typical 2D projections of drilling particle shape (Classified degree of circularity is noted under each image).

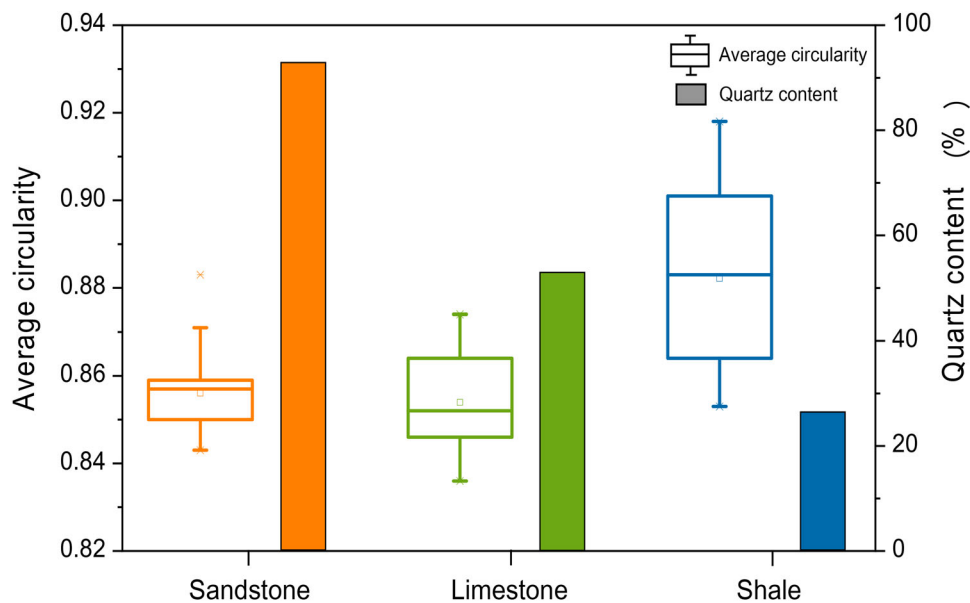
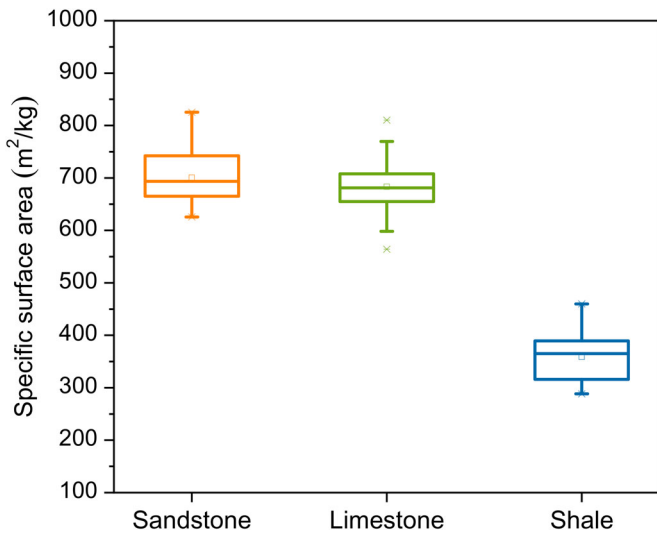


Figure 6. Statistics of average circularity and quartz content for particles recovered from all tests on the three rocks.

limestone as approximately double that recorded for shale (Figure 7). As the same particle mass is collected, the specific surface area has a direct relation to the total surface area which is affected by the quantity and circularity of particles. For a certain particle, a higher circularity is linked to a smaller surface area. Figure 8 shows contrasts in the volume proportions of each particle fraction, which reflects contrasts in the quantity of that particular rock. The mean value of circularity for the three types of rock particles is shown in Figure 9.

The similar quantities and circularities of the sandstone and limestone particles may explain their similar characteristics of specific surface area. But Figure 8 indicates that fine particles of shale are less abundant than those of sandstone and limestone, with more medium particles and similar numbers of coarse particles. Considering the higher mean circularity of shale particles (Figure 9), the total surface area of shale particles is considerably smaller than that of the sandstone and limestone particles, and thus shale particles exhibit the smallest specific surface area.



**Figure 7.** Statistics of specific surface area for rock particles recovered from the three rocks for all tests.

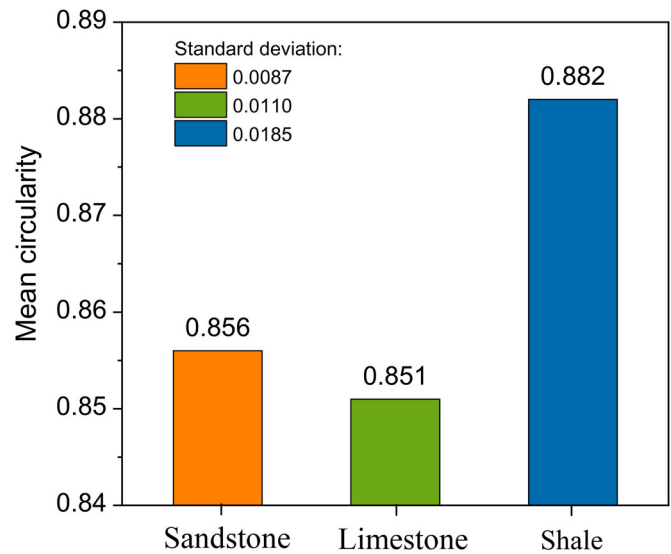


**Figure 9.** Mean value of particle circularity from all tests for the three rocks.

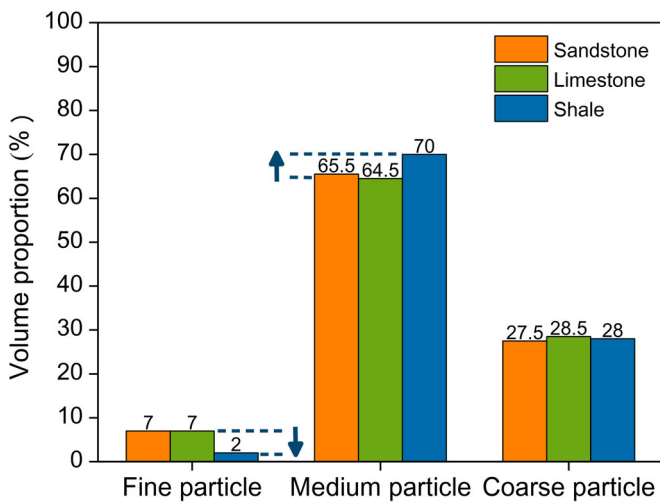


**Figure 8.** Volume proportions of particle size fractions recovered from all tests for the three rocks.

#### 4. Conclusion

Factors that influence particle size distribution (PSD), average circularity and specific surface area in particles produced in rock drilling are investigated through drilling experiments on sandstone, limestone, and shale. The basic conclusions can be drawn as follows:

1. The effects of impact breakage and contact abrasion caused by the interaction between particles are the main factors influencing modes of particle size and shape. Impact breakage may decrease both particle size and circularity, with contact abrasion increasing particle circularity. Impact breakage is affected by the structural distribution of mineral phases, while contact abrasion is conditioned by the hardness of the mineral phases. A two-phase structure promotes impact breakage over an homogeneous structure, with the presence of low-hardness phases promoting contact abrasion.

2. The particle size distribution (PSD) is affected by the structural distribution of the mineral phases. Rock with an homogeneous structure (shale) are uniform and compact, resist impact breakage, with the result that drilling particles converge in a single coarse fraction with the PSD showing a single peak. Conversely, two-phase structure rocks (limestone and sandstone) are prone to break into two sets of particles with different hardnesses. Here, the soft and hard particles converge to fine and coarse fractions, respectively and the resulting PSD is bimodal.

3. The average circularity of the drilling particles is mainly affected by the hardness of the mineral phases. High content of low hardness phases may increase the average circularity. Chemical transformations of certain phases may decrease hardness thereby increasing the circularity. This may result in shales where oxidized pyrite increases particle circularity. The range in average particle circularity is determined by the high-hardness phases. Higher content of high-hardness phases (quartz) reduces the range in average particle circularity.

4. The specific surface area of the particles is determined by the structural distribution and hardness of the mineral phases which directly affect the quantity and roundness of the breaking particles. Furthermore, compared to rocks with a two-phase structure (sandstone and limestone), rock with an homogeneous structure and low average hardness of the phases (shale) develops a lower specific surface area.

#### Disclosure statement

No potential conflict of interest was reported by the authors.

#### Funding

This work is supported by the National Natural Science Foundation of China (Nos. 51674122 and 51874310).

## References

- Akhshik, S., M. Behzad, and M. Rajabi. 2016. CFD-DEM Simulation of the Hole Cleaning Process in a Deviated Well Drilling: The Effects of Particle Shape. *Particology* 25: 72–82. doi:10.1016/j.partic.2015.02.008.
- Bondarenko, V. P., I. V. Andreyev, I. V. Savchuk, O. O. Matviichuk, O. V. Ievdokymova, and A. V. Galkov. 2013. Recent Researches on the Metal-Ceramic Composites Based on the Decamicon-Grained WC. *International Journal of Refractory Metals and Hard Materials* 39: 18–31. doi:10.1016/j.ijrmhm.2013.01.018I.
- Che, D., W. Zhu, and K. F. Ehmann. 2016. Chipping and Crushing Mechanisms in Orthogonal Rock Cutting. *International Journal of Mechanical Sciences* 119: 224–236. doi:10.1016/j.ijmecsci.2016.10.020I.
- Dunatunga, S., and K. Kamrin. 2017. Continuum Modeling of Projectile Impact and Penetration in Dry Granular Media. *Journal of the Mechanics and Physics of Solids* 100: 45–60. doi:10.1016/j.jmps.2016.12.002I.
- Ersoy, A., and M. D. Waller. 1997. Drilling Detritus and the Operating Parameters of Thermally Stable PDC Core Bits. *International Journal of Rock Mechanics and Mining Sciences and Sciences* 34 (7): 1109–1123. 365-1609(97)90203-3. doi:10.1016/s1.
- Fei, W., G. A. Narsilio, and M. M. Disfani. 2019. Impact of Three-Dimensional Sphericity and Roundness on Heat Transfer in Granular Materials. *Powder Technology* 355: 770–781. doi:10.1016/j.powtec.2019.07.094I.
- Flegner, P., J. Kačur, M. Durdán, M. Laciak, B. Stehlíková, and M. Pástor. 2016. Significant Damages of Core Diamond Bits in the Process of Rocks Drilling. *Engineering Failure Analysis* 59: 354–365. doi:10.1016/j.engfailanal.2015.10.016I.
- Guzzo, P. L., A. A. Tino, and J. B. Santos. 2015. The Onset of Particle Agglomeration during the Dry Ultrafine Grinding of Limestone in a Planetary Ball Mill. *Powder Technology* 284: 122–129. doi:10.1016/j.powtec.2015.06.050I.
- Harper, T. R., and J. L. Chambers. 2004. Stress State and Its Influence on Drilling Performance in the Brighton Marine Field, Trinidad. *Marine and Petroleum Geology* 21 (7): 947–963. doi:10.1016/j.marpetgeo.2004.02.005I.
- Krauthammer, T., M. M. Elfahal, J. Lim, T. Ohno, M. Beppu, and G. Markeset. 2003. Size Effect for High-Strength Concrete Cylinders Subjected to Axial Impact. *International Journal of Impact Engineering* 28 (9): 1001–1016. 34-743x(02)00166-5I. doi:10.1016/s07.
- Liu, K., X. Xie, Z. Luo, Q. Hu, and C. Huang. 2016. Full-Scale Field Load Testing of Long Drilled Shafts with Enlarged Base Constructed in Marine Sediment. *Marine Georesources & Geotechnology* 35 (3): 346–356. 72684I. doi:10.1080/1064119x.2016.11.
- Luo, J., G. Huang, L. Zhang, F. Huang, and J. Zheng. 2018. Micro Shape of Coal Particle and Crushing Energy. *International Journal of Mining Science and Technology* 28 (6): 1009–1014. doi:10.1016/j.ijmst.2018.03.001I.
- Miyazaki, K., T. Ohno, H. Karasawa, S. Takakura, and A. Eko. 2016. Performance Evaluation of Polycrystalline Diamond Compact Percussion Bits through Laboratory Drilling Tests. *International Journal of Rock Mechanics and Mining Sciences* 87: 1–7. doi:10.1016/j.ijrmms.2016.04.020I.
- Nascimento, D. R., B. R. Oliveira, V. G. P. Saide, S. C. Magalhães, C. M. Scheid, and L. A. Calçada. 2019. Effects of Particle-Size Distribution and Solid Additives in the Apparent Viscosity of Drilling Fluids. *Journal of Petroleum Science and Engineering* 182: 106275. doi:10.1016/j.petrol.2019.106275I.
- Pellegrin, D. V., N. D. Corbin, G. Baldoni, and A. A. Torrance. 2009. Diamond Particle Shape: Its Measurement and Influence in Abrasive Wear. *Tribology International* 42 (1): 160–168. doi:10.1016/j.triboint.2008.04.007I.
- Reddish, D. J., L. R. Stace, P. Vanichkobchinda, and D. N. Whittles. 2005. Numerical Simulation of the Dynamic Impact Breakage Testing of Rock. *International Journal of Rock Mechanics and Mining Sciences* 42 (2): 167–176. doi:10.1016/j.ijrmms.2004.06.004I.
- Ren, X., H. Miao, and Z. Peng. 2013. A Review of Cemented Carbides for Rock Drilling: An Old but Still Tough Challenge in Geo-Engineering. *International Journal of Refractory Metals and Hard Materials* 39: 61–77. doi:10.1016/j.ijrmhm.2013.01.003I.
- Spagnoli, G., C. Bosco, and P. Oreste. 2016. Geotechnical and Machinery Properties Influencing the Offshore Pile Drillability. *Marine Georesources & Geotechnology* 35 (2): 266–274. doi:10.1080/1064119x.2016.1155189I.
- Tavares, L. M. 1999. Energy Absorbed in Breakage of Single Particles in Drop Weight Testing. *Minerals Engineering* 12 (1): 43–50. doi:10.1016/S0892-6875(98)00118-6.
- Tavares, L. M. 2004. Optimum Routes for Particle Breakage by Impact. *Powder Technology* 142 (2–3): 81–91. doi:10.1016/j.powtec.2004.03.014I.
- Weichert, R. 1991. Theoretical Prediction of Energy-Consumption and Particle-Size Distribution in Grinding and Drilling of Brittle Material. *Particle & Particle Systems Characterization* 8 (1): 55–62. doi:10.1016/0141-6359(91)90083-u.
- Whittles, D. N., S. Kingman, I. Lowndes, and K. Jackson. 2006. Laboratory and Numerical Investigation into the Characteristics of Rock Fragmentation. *Minerals Engineering* 19 (14): 1418–1429. doi:10.1016/j.mineng.2006.02.004I.
- Wu, J., and R. D. Han. 2009. A New Approach to Predicting the Maximum Temperature in Dry Drilling Based on a Finite Element Model. *Journal of Manufacturing Processes* 11 (1): 19–30. doi:10.1016/j.jmappro.2009.07.001I.
- Xu, Y., J. Yang, H. Xiang, W. Meng, and H. Deng. 2018. Calculation of Side Friction Resistance between the Formation and Conductor during the Jetting Process in Deepwater Drilling. *Marine Georesources & Geotechnology* 37 (4): 409–416. doi:10.1080/1064119x.2016.1236860I.
- You, L., Q. Tan, Y. Kang, X. Zhang, C. Xu, and C. Lin. 2018. Optimizing the Particle Size Distribution of Drill-in Fluids Based on Fractal Characteristics of Porous Media and Solid Particles. *Journal of Petroleum Science and Engineering* 171: 1223–1231. doi:10.1016/j.petrol.2018.08.051I.
- Zhou, Y., W. Zhang, I. Gamwo, and J. Lin. 2017. Mechanical Specific Energy versus Depth of Cut in Rock Cutting and Drilling. *International Journal of Rock Mechanics and Mining Sciences* 100: 287–297. doi:10.1016/j.ijrmms.2017.11.004I.